HHS Public Access

Author manuscript

Hepatology. Author manuscript; available in PMC 2017 October 01.

Published in final edited form as:

Hepatology. 2016 October ; 64(4): 1302–1316. doi:10.1002/hep.28713.

Endothelial Notch signaling is essential to prevent hepatic vascular malformations in mice

Henar Cuervo[#1,4], **Corinne M. Nielsen**[#1], **Douglas A. Simonetto**[2], **Linda Ferrell**[3], **Vijay H. Shah**[2], and **Rong A. Wang**[1,*]

[1]Laboratory for Accelerated Vascular Research, Department of Surgery, University of California, San Francisco, San Francisco, CA

[2]Division of Gastroenterology and Hepatology, Mayo Clinic, Rochester, MN

[3]Department of Pathology, University of California, San Francisco, San Francisco, CA

[#] These authors contributed equally to this work.

Abstract

Liver vasculature is crucial for adequate hepatic functions. Global deletion of Notch signaling in mice results in liver vascular pathologies. However, whether Notch in endothelium is essential for hepatic vascular structure and function remains unknown. To uncover the function of endothelial Notch in the liver, we deleted Rbpj, a transcription factor mediating all canonical Notch signaling, or Notch1, specifically from the endothelium of postnatal mice. We investigated the hepatic vascular defects in these mutants. The liver was severely affected within two weeks following endothelial deletion of Rbpj from birth. Two-week old mutant mice had enlarged vessels on the liver surface, abnormal vascular architecture, and dilated sinusoids. Vascular casting and fluorosphere passage experiments indicated the presence of porto-systemic shunts. These mutant mice presented severely necrotic liver parenchyma and significantly larger hypoxic areas, likely resulting from vascular shunts. We also found elevated levels of VEGF receptor 3 together with reduced levels of ephrin-B2, suggesting a possible contribution of these factors to the generation of hepatic vascular abnormalities. Deletion of Rbpj from the adult endothelium also led to dilated sinusoids, vascular shunts, and necrosis albeit milder than that in mice with deletion from birth. Similar to deletion of Rbpj, loss of endothelial Notch1 from birth led to similar hepatic vascular malformations within two weeks.

Conclusions—Endothelial Notch signaling is essential for the development and maintenance of proper hepatic vascular architecture and function. Our findings may help understand the molecular pathogenesis of hepatic vascular malformation and the safety of therapeutics inhibiting Notch.

Keywords

liver vasculature; vascular malformations; Rbpj

[*]**Corresponding author:** Rong A. Wang, PhD, University of California, San Francisco, HSW 1618, 513 Parnassus Avenue, San Francisco, CA 94143, Fax: 415-353-4370, Phone: 415-476-6855, rong.wang@ucsf.edu.

[4]Current address: Department of Physiology and Biophysics, University of Illinois Chicago, College of Medicine, Chicago, IL.

The liver has a wide range of functions key for organismal homeostasis, including blood detoxification and lipid metabolism, and the presence of a proper vasculature is critical for its performance. Most vascular diseases of the liver are rare; however, without timely diagnosis, they can lead to significant morbidity and mortality(1). Hepatic vascular malformations (HVMs), characterized by the abnormal shunting of liver blood vessels, are such lesions. In patients, while HVMs can be idiopathic or acquired as a consequence of underlying cirrhosis, liver injury or hepatocellular carcinoma, most cases are congenital, as in hereditary hemorrhagic telangiectasia (HHT)(2). The incidence of HVM detection is rising, in part due to increased use of ultrasonography or other liver imaging assays in patients.

The liver receives blood from two sources (the hepatic artery and the portal vein), increasing the classes of vascular shunts that can develop. Shunts may be: 1) arteriovenous shunts linking the hepatic artery and the hepatic vein, 2) porto-systemic shunts between the portal vein and the hepatic vein, and 3) arterioportal shunts connecting the hepatic artery and the portal vein. Any or all of these shunt classes can form in a given liver(1). Clinical manifestation of HVMs is affected by the type and degree of blood shunting, and symptoms can include high-output heart failure, portal hypertension, hepatic encephalopathy, and biliary ischemia(1). A better understanding of the molecular pathways that govern the function of liver vasculature will aid in the diagnosis and treatment of these liver vascular pathologies.

The highly conserved Notch signaling pathway is involved in many developmental and pathological processes, including the establishment of arterial EC identity and in the regulation of the angiogenic response(3),(4). Upon ligand binding, the Notch receptor undergoes a cascade of proteolytic cleavages that results in the release of its intracellular domain (ICD). The Notch ICD translocates to the nucleus, where it binds to the transcription factor Rbpj (recombination signal binding protein for immunoglobulin kappa J region), and activates the transcription of target genes. Though mammals have four Notch receptors (Notch1-4), endothelial cells (ECs) predominantly express Notch1 and Notch4(4). Mice lacking Notch4 do not develop an overt phenotype, while mice deficient for Notch1 present arrested growth and die at embryonic stages with severe vascular anomalies(5). Hence, Notch1 is considered to be the main Notch receptor in the endothelium; however, deletion of both Notch1 and Notch4 results in a more pronounced phenotype than that of Notch1 alone(5), suggesting synergistic functions of the receptors.

The Notch signaling pathway has been identified as a regulator of liver vasculature maintenance. Mice with deletion of Notch1 develop hepatic vascular tumors(6, 7), while deletion of Rbpj in mice results in venooclusive disease(8). These loss of function studies were performed via non cell-specific ablation of Notch signaling. To elucidate the role of Notch signaling specifically in the endothelium, we have used mice with endothelial deletion of Rbpj (to delete signaling via both endothelial Notch receptors) or Notch1 at different growth stages. Our results indicate a critical role for endothelial Notch signaling in the maintenance of liver sinusoid architecture and functionality and in the prevention of HVMs.

MATERIALS & METHODS

Mouse Experiments

Animal experiments were performed in compliance with the University of California, San Francisco (UCSF) Institutional Animal Care and Use Committee (IACUC) guidelines under animal protocols AN085404 and AN102764. All animals received humane care according to the criteria outlined in the "Guide for the Care and Use of Laboratory Animals" prepared by the National Academy of Sciences and published by the National Institutes of Health (NIH publication 86-23 revised 1985).

Rbpj$^{flox/flox}$(9), *Cdh5(PAC)-CreERT2*(10), *Rosa26*$^{mT/mG}$ (*mT/mG*)(11), *Notch1*$^{flox/flox}$(12), and *ephrin-B2*$^{tau\text{-}lacZ}$(13) mice were obtained from T. Honjo (Kyoto University, Japan), R. Adams (Max Planck Institute for Molecular Biomedicine, Münster, Germany), L. Luo (Stanford University, California, USA), F. Radtke (École Polytechnique Fédéral de Lausanne, Switzerland), and D. Anderson (California Institute of Technology, USA), respectively.

Detailed methods for Cre activation, histology, immunostaining, βgal detection, two-photon microscopy, vascular shunting assay, portal pressure measurement, liver panel markers, LSEC enrichment, real-time PCR, time-lapse imaging, and statistical analysis are included in the Supporting Information.

RESULTS

Vascular shunts develop in postnatal Rbpj$^{i\Delta EC}$ mice

To interrogate the role of Notch signaling in the liver endothelium, we deleted *Rbpj*, which encodes the Rbpj transcription factor downstream of Notch and essential for canonical Notch signaling(3). Endothelial deletion of *Rbpj* was mediated by tamoxifen-inducible Cre-recombinase activity driven by the *vascular endothelial (VE)-Cadherin* (*Cadherin5*) promoter in *Rbpj*$^{flox/flox}$*; Cdh5(PAC)-CreERT2* mice (Rbpj$^{i\Delta EC}$). Inclusion of the *mT/mG* reporter(11) allowed us to monitor Cre-recombinase activity and to visualize ECs. Tamoxifen injection of Rbpj$^{i\Delta EC}$ mice at postnatal day (P)1 and P2 resulted in absence of Rbpj specifically in the ECs of the liver (Fig.S1a,b,c). mGFP expression in Rbpj$^{i\Delta EC}$ mice bearing *mT/mG* was observed throughout the liver endothelium at P14 (Fig. S1d) and throughout the vessels of the retina, where we observed a dramatic increase in retinal angiogenesis at P7 (Fig.S1e,f), consistent with previous reports(14, 15). Taken together, these results indicate specific, efficient endothelial deletion of Rbpj in our mouse model, including the liver vessels.

Analysis of P14 Rbpj$^{i\Delta EC}$ pups revealed a dramatically affected liver. Gross examination revealed enlarged vessels on the liver surface, particularly along lobe edges. Importantly, large swathes/regions of the hepatic parenchyma were discolored (Fig. 1a,b). Liver sections revealed the presence of dilated sinusoids in Rbpj$^{i\Delta EC}$ pups (Fig.1c,d and Fig.S2). Sinusoid dilation, most prominent around the central venules, was significantly increased in Rbpj$^{i\Delta EC}$ mice, when compared with heterozygous and wild type control littermates (Fig.1e). Perturbations to normal sinusoid morphology were severe enough to interrupt normal

hepatic plate architecture. Moreover, enlarged sinusoids were observed connecting the portal and the central venules directly (Fig.1c,d), suggesting the formation of vascular shunts. To gain a deeper understanding of these vessel irregularities, we performed casting of the liver vasculature. When casting resin was injected in the left ventricle of controls, the arterial and portal vascular branches were filled (Fig.2a). The density of the resin prevented penetration of the sinusoids of healthy livers. However, when Rbpj$^{i\Delta EC}$ mice were injected with the resin, both the portal branches and the central venules were filled, indicating abnormal shunting between these two vascular systems (Fig.2b).

To further demonstrate the presence of vascular shunts, we analyzed the circulation pattern of size-limiting (15μm) microspheres. FITC-conjugated beads, injected into the portal vein of P14 control mice, were arrested in the liver (Fig.2c). In Rbpj$^{i\Delta EC}$ mice, the beads bypassed liver sinusoids and lodged in the lungs (Fig.2d), indicating the presence of porto-systemic vascular shunts. Taken together, these data suggest that Rbpj$^{i\Delta EC}$ mice develop vascular abnormalities that lead to the formation of vascular shunts.

Endothelial loss of Rbpj at birth results in liver necrosis, malfunction and hypoxia by P14

Histological analysis of liver, hematoxylin and eosin (H&E) sections, revealed dilated sinusoids and expanded subcapsular sinuses, consistent with the enlarged vessels seen near the liver surface. Additionally, a variable degree of hepatocyte damage, ranking from atrophy to severe panacinar necrosis, was observed in severe cases, forming an arc following the zone typical of ischemic injury in the milder injuries (Fig.3a,b and Fig.S3a,b).

The porto-systemic shunting and abnormal vessel structure in Rbpj$^{i\Delta EC}$ mice led us to hypothesize that liver necrosis might result from poor tissue oxygenation. To test this, P14 Rbpj$^{i\Delta EC}$ pups were injected with pimonidazole hydrochloride (Hypoxyprobe-1), which binds to hypoxic tissue. To visualize the vascular perfusion of the liver, mice were co-injected with FITC conjugated *Lycopersicon esculentum* lectin. Immunostaining against Hypoxyprobe-1 showed significantly increased hypoxic area in Rbpj$^{i\Delta EC}$ mice when compared to the heterozygous control (Fig.3c,d,e). Of note, hypoxic areas in Rbpj$^{i\Delta EC}$ mice corresponded to regions with reduced lectin perfusion.

Because of the high levels of necrosis and hypoxia observed, we hypothesized that liver function was impaired in these mice. Rbpj$^{i\Delta EC}$ mice presented higher serum levels of bilirubin, alanine transaminase (ALT), aspartate transaminase (AST), and alkaline phosphatase, as well as lower levels of total protein and albumin (Fig.S4), suggesting that Rbpj$^{i\Delta EC}$ mice have a poorly perfused liver vasculature that results in hypoxia, liver damage and malfunction.

Because previous work using global Notch1 or Rbpj deletion reported increased EC proliferation, we investigated the livers of Rbpj$^{i\Delta EC}$ mice at P7, before the onset of severe necrosis. Phospho-histone-H3 immunostaining appeared increased in Rbpj$^{i\Delta EC}$ liver ECs; however, this difference was not statistically significant (Fig.3f, Fig.S5), suggesting that increased endothelial proliferation does not contribute to the vascular phenotypes observed in P14 Rbpj$^{i\Delta EC}$ mice.

Endothelial deletion of *Rbpj* in adult mice also induces vascular shunts

To determine whether the vascular defects following loss of endothelial Rbpj were age dependent, we deleted *Rbpj* by injecting tamoxifen in 6 week-old mice and analyzed the liver vasculature 6 weeks later (adult Rbpj$^{i\Delta EC}$). We found Rbpj efficiently and specifically deleted in the adult liver endothelium at this time point (Fig.S6a,b). Similarly, mGFP expression derived from the *mT/mG* reporter was observed throughout the adult liver vasculature (Fig.S6d,e).

Adult Rbpj$^{i\Delta EC}$ mice presented enlarged vessels on the liver surface (Fig.4a); however, this phenotype was not as severe as that observed following endothelial *Rbpj* deletion from birth. Similarly, adult Rbpj$^{i\Delta EC}$ showed a modest discoloration of the liver parenchyma, while the discoloration following endothelial *Rbpj* deletion from birth was more pronounced. Consistently, histological analysis of the liver from adult Rbpj$^{i\Delta EC}$ mice revealed less robust sinusoid dilation (Fig.4b). Hepatocyte atrophy was observed following the same arc pattern present in the necrotic hepatocytes of mice with loss of endothelial *Rbpj* form birth, indicative of a milder ischemic insult in the adult mice. Also, wide plates of hepatocytes with a nodular regenerative hyperplasia (NRH)-like appearance were noticed (Fig.4b and Fig.S7).

Further analysis also showed an abnormal vascular architecture (Fig.4c). Quantification of sinusoid width around central venules demonstrated that sinusoids significantly wider than heterozygous controls (Fig.4d), consistent with that observed following *Rbpj* deletion at birth.

To determine whether deletion at 6 weeks also led to vascular shunting, we injected fluorescent microspheres in the portal vein. Microspheres were lodged in the liver of control mice, while no beads were observed in the lungs (Fig.5a). In adult Rbpj$^{i\Delta EC}$ mice, most of the microspheres passed through the liver vasculature and were detected in the lungs, demonstrating direct porto-systemic shunting (Fig.5b). Altogether, these results indicate that while the liver phenotype is less severe than deletion at birth, endothelial deletion of *Rbpj* at 6 weeks also results in direct porto-systemic shunting.

Endothelial deletion of *Rbpj* in adult mice leads to increased portal pressure

The observation that mice with adult deletion of *Rbpj* develop a NRH-like phenotype led us to consider the possibility that these mice also present increased portal pressure. Direct measurement of portal pressure showed significantly increased values in Rbpj$^{i\Delta EC}$ mice when compared to control (Fig.5c). Similarly, a significantly increased spleen/body weight ratio, an indirect surrogate of elevated portal pressure was observed in Rbpj$^{i\Delta EC}$ mutants (Fig.5d). In the absence of observed liver fibrosis on histology, these results are suggestive of presinusoidal portal hypertension, as commonly encountered in nodular regenerative hyperplasia, in Rbpj$^{i\Delta EC}$ mice. We cannot rule out, however, that hemodynamic changes resulting from other abnormalities in Rbpj$^{i\Delta EC}$ mice(16) contribute to the nodular phenotype, and the elevated portal pressure observed in these mice.

Endothelial deletion of *Notch1* at birth resembles that of *Rbpj*

Since Rbpj mediates canonical Notch signaling, we have used it as a proxy to interrogate the role of Notch signaling in the liver vasculature; however, to confirm that the phenotypes we observed following *Rbpj* deletion reflect loss of canonical Notch signaling, we investigated the role of the Notch1 in the liver vasculature. *Notch1*$^{flox/flox}$; *Cdh5(PAC)-CreERT2* (Notch1$^{i\Delta EC}$) mice were injected with tamoxifen at birth, and the liver vasculature was analyzed at P14. Successful and efficient Notch1 deletion was verified (Fig.S8).

Similar to that observed in P14 Rbpj$^{i\Delta EC}$, Notch1$^{i\Delta EC}$ mice had enlarged vessels on the liver surface as well as hepatic discoloration, though these phenotypes were milder than those observed in Rbpj$^{i\Delta EC}$ mice (Fig.6a,b). When the vascular organization was analyzed, liver sinusoids appeared dilated around the central vein area. As observed in Rbpj$^{i\Delta EC}$ mice, the architecture and disposition of these vessels was severely altered, suggesting direct shunting between the portal and central veins (Fig.6c,d).

To determine whether Notch1$^{i\Delta EC}$ mice also develop porto-systemic shunts, we injected fluorescent microspheres into the portal vein. Lungs from control mice lacked microspheres, which were retained in the liver sinusoids (Fig.6e). In contrast, the lungs of Notch1$^{i\Delta EC}$ mice contained microspheres (Fig.6f), indicating the presence of vascular shunts. Taken together, these data show that loss of Notch1 receptor function at birth in ECs recapitulates the phenotypes observed in Rbpj$^{i\Delta EC}$ mice.

Given that previous publications have reported the development of NRH and angiosarcoma in the liver, following global deletion of Notch1, we explored the longer-term effects of endothelial Notch1 deletion. Survival of Notch1$^{i\Delta EC}$ and control mice was monitored up to 80 days after birth, with no significant differences observed (Fig.S9c). Additionally, we evaluated H&E sections from P80 Notch1$^{i\Delta EC}$ mice and found dilated sinusoids and slight differences in hepatocyte size between the portal and central regions (Fig.S9a,b). However, we did not observe the NRH-like phenotype detected in adult Rbpj$^{i\Delta EC}$, and we found no evidence of vascular tumors. These results indicate that long-term endothelial deletion of Notch1 from birth does not result in similar liver parenchymal abnormalities to those of Rbpj$^{i\Delta EC}$, or liver vascular tumors, within this timeframe.

Endothelial deletion of *Rbpj* leads to abnormalities in isolated liver sinusoid endothelial cells

To gain cell biological insight into the role of endothelial Notch signaling in the liver vasculature, we isolated liver sinusoid endothelial cells (LSECs) from Rbpj$^{i\Delta EC}$ and control mice at P7, to avoid secondary effects that might result from the hypoxia and hepatocyte necrosis observed in P14 Rbpj$^{i\Delta EC}$ mice. We imaged isolated cells every 15min for 48h under culture conditions. We evaluated the rate of cell proliferation and cell death of LSECs from Rbpj$^{i\Delta EC}$ and found no significant differences when compared to controls (FigS10a,b). However, Rbpj$^{i\Delta EC}$ LSECs exhibited an abnormal cell:cell interface that acquired the appearance of membranous “holes” (Movies 1,2). Consistent with time-lapse imaging, isolated and fixed LSECs showed an increased number of membranous “holes” per cell (Fig. 7a,b,c). Interestingly, a similar aberrant cell-cell interface was observed in liver sections in

the sinusoids of adult Rbpj$^{i\Delta EC}$ mice (Fig.7a,b). These results suggest that endothelial Rbpj may be involved in regulating endothelial cellular properties that affect EC:EC interactions in the liver.

Endothelial deletion of *Rbpj* leads to downregulation of *ephrin-B2*

We investigated molecular changes to liver endothelium, following endothelial deletion of Rbpj using freshly isolated LSECs from P7 Rbpj$^{i\Delta EC}$ and control mice. We first evaluated Notch downstream genes, including the arterial marker *ephrin-B2* and the venous marker *Ephb4*, previously described to be modulated by Notch in the liver endothelium liver(6, 17) and involved in AVM formation in the brain(18). While *Ephb4* was not altered significantly, *ephrin-B2* was significantly reduced in LSECs from P7 Rbpj$^{i\Delta EC}$ mice, when compared to control (Fig.7f).

We also evaluated expression of candidate genes previously shown to be regulated by Notch and involved in vascular shunting, *Matrix Gla protein*(19), *Smad4*(20), and *Pten*(21). We did not observe significant changes in the levels of these genes (Fig.7f), indicating that modulation of these pathways is not likely involved in the formation of porto-systemic shunts, following endothelial deletion of Rbpj.

We further investigated expression of ephrin-B2 *in vivo* by crossing Rbpj$^{i\Delta EC}$ mice with a mouse line carrying *lacZ* under the control of the *ephrin-B2* promoter (*ephrin-B2*$^{tau\text{-}lacZ}$). In control mice, β-galactosidase (produced by *ephrin-B2*$^{tau\text{-}lacZ}$) was detected in the arteries, portal venules, and some periportal sinusoids (Fig.7d); however, Rbpj$^{i\Delta EC}$-*ephrin-B2*$^{tau\text{-}lacZ}$ mice showed drastically reduced levels of the reporter (Fig.7e). These results suggest a possible role for ephrin-B2 in the development of porto-systemic shunts, following endothelial loss of Notch signaling.

Loss of endothelial Notch signaling results in upregulation of VEGFR3 in dilated sinusoids

Recent studies have shown that the hyper-angiogenic response observed in postnatal retina in Notch loss-of-function mice is mainly mediated by VEGFR3(22). We therefore hypothesized that Rbpj$^{i\Delta EC}$ livers would have altered VEGFR3 expression. mRNAs from the livers of P14 mice were analyzed by RT-PCR, and *Vegfr3* (*Flt4*), but not its ligands *Vegfc* and *Vegfd*, was found significantly increased in Rbpj$^{i\Delta EC}$ mice (Fig.8a). Interestingly, *Flt4* levels in P7 LSECs did not show significant differences between Rbpj$^{i\Delta EC}$ and control mice (Fig.S11a).

Immunostaining demonstrated that VEGFR3 was highly upregulated in P14 and P7 Rbpj$^{i\Delta EC}$ liver vessels. This upregulation was most pronounced in the sinusoids nearest the central venule, where sinusoid dilation is maximal (Fig.8b,c,d,e). Consistent with these data, VEGFR3 upregulation was observed in the sinusoids of P14 Notch1$^{i\Delta EC}$ mice (Fig.S12). Immunostaining against VEGFR2 revealed no differences in Rbpj$^{i\Delta EC}$ vs. control mice (Fig.S13). Similarly, *Kdr* (*Vegfr2*) levels in P7 LSECs of Rbpj$^{i\Delta EC}$ mice were not significantly different than Controls (Fig.S11b). Together, these results suggest a post-transcriptional regulation of VEGFR3 by Notch signaling in liver sinusoids and that VEGFR3 may be involved in the development of vascular anomalies, following endothelial Notch loss of function.

DISCUSSION

Here, we show for the first time that endothelial deletion of Notch signaling results in HVMs

While previous studies have reported similar vascular and parenchymal phenotypes in the liver, following global deletion of Notch during adulthood(23), our results delineate that impaired Notch signaling in the endothelial lineage is responsible for the observed hepatic abnormalities. Disruptions to liver parenchyma and sinusoid architecture and impairments to liver function were very severe following loss of endothelial Notch function in immature mice, but were milder when endothelial Notch signaling was deleted during adulthood, suggesting differential temporal regulation of Notch. Additionally, VEGFR3 was increased in the abnormal sinusoids of Notch mutant mice, and *ephrin-B2* was reduced, suggesting that these factors are involved in the formation of liver vascular malformations. Together, these results support a role for Notch in postnatal liver endothelium to establish adequate density and interface of the hepatic vasculature (Fig.S14).

Endothelial Notch signaling regulates sinusoid diameter and prevents porto-systemic shunting

Loss of Notch signaling in ECs leads to dilated sinusoids, originating around the central vein area, that ultimately form direct shunts between the portal and central veins and result in the development of HVMs. Increased liver sinusoid diameter has also been reported in mice with non-specific loss of Notch1(6) and in mice treated with antibodies against the Notch ligand Dll4(24). Observations in other vascular beds, such as the developing retina, support a role for endothelial Notch in regulating vessel diameter. Increased diameter of venule branches was observed in $Rbpj^{i\Delta EC}$ mice(15, 16). Additionally, endothelial Notch was reported to regulate vessel diameter in the yolk sac(25).

In the retina(15) and in liver sinusoids(6), increased vessel diameter is consistent with increased angiogenesis and hypervascularity, triggered by loss of Notch signaling. It is likely that, in the presence of a hypervascular network generated by loss of endothelial Notch signaling, the enlarged sinusoids form as a consequence of increased angiogenesis. In these settings, blood flow through the liver will opt for the path of least resistance within the wider, non-remodeled, sinusoids, selecting for their growth at the expense of neighboring branches. As sinusoid dilation and porto-systemic shunting progress, tissue perfusion and oxygenation is impaired, as evidenced by increased hypoxia in mutant livers. Consistent with this, similar hemodynamic changes, caused by enlarged vessel diameter, contribute to the development of vascular malformations in two different models of brain AVMs(26, 27). Progressive, steal-mediated enlargement of liver sinusoids in mice with loss of endothelial Notch may similarly lead to the development of vascular malformations. Together, our data suggest that endothelial Notch regulates sinusoid diameter and prevents porto-systemic shunting in the postnatal liver.

The phenotypes resulting from the ablation of *Rbpj* reveal temporal differences in Notch signaling

Our results suggest a critical role for endothelial Notch in the early postnatal liver. Endothelial ablation of Notch signaling at this time results in a disruption of the developing vascular network that rapidly leads to severe HVMs and liver malfunction. Meanwhile, deletion of Notch in mature mice requires more time for the appearance of HVMs. These results suggest that endothelial Notch regulates liver vasculature in a temporally controlled manner. This temporal discrepancy is likely due to the quiescent state of the adult vasculature, wherein ECs are not exposed to the myriad of angiogenic stimuli present in the early postnatal liver. This age-dependent phenotype is consistent with the previous proposition that an active angiogenic environment is key for the development of vascular malformations(28, 29).

Notch4, in addition to Notch1, may be required in ECs to prevent HVMs

Endothelial *Rbpj* deletion results in more severe liver vascular malformations than endothelial deletion of *Notch1*. Because ablation of Rbpj impairs all canonical Notch signaling, it is possible that other Notch receptors are important. Since Notch4 is expressed in ECs, it is possible that Notch4 deficiency, in concert with Notch1 deficiency, is required for liver vascular malformations. Indeed, deletion of both *Notch1* and *Notch4* in embryos results in a more pronounced phenotype than that of *Notch1* deletion alone(5). Importantly, mice lacking Rbpj also die at embryonic stages and display similar defects to those of the Notch1/Notch4 double knockouts(30). Therefore, it is likely that the increased severity of hepatic vascular malformations in Rbpj$^{i\Delta EC}$ livers, as opposed to Notch1$^{i\Delta EC}$ livers, results from loss of Notch signaling via both Notch1 and Notch4 receptors. However, Rbpj has been reported to act independently of Notch signaling(31). Thus it is also possible that non-Notch mediated effects of Rbpj are important in preventing porto-systemic shunting.

VEGFR3 upregulation in endothelium of Rbpj mutants supports a role in HVM formation

Our results show an upregulation of VEGFR3 but not its ligands in mice with endothelial deletion of Notch signaling. VEGFR3 staining was more robust in the sinusoids associated with the central vein area, where the vascular abnormalities are first detected and more severe. Surprisingly, we did not see a difference in the VEGFR2 levels, consistent with the work of Dill et al.(6) who detected no changes in the *Vegfr2* levels from *Notch1*^{null} sinusoid ECs, and also with the lack of change in VEGFR2 albeit upregulation of VEGFR3 in the lung and developing retina of Rbpj$^{i\Delta EC}$ mice(6). Interestingly, we observed no differences in levels of *Vegfr3* mRNA in P7 isolated LSECs. Similar uncoupled regulation of mRNA and protein levels of VEGFR3 was also observed by Benedito et al.(22) who concluded that Notch likely regulates VEGFR3 by additional post transcriptional mechanisms. These studies also conclude that VEGFR3 kinase activity (as opposed to the ligand binding domain) mediates deregulated angiogenesis in settings where Notch activity is low or absent(22), consistent with the vascular abnormalities seen in Rbpj$^{i\Delta EC}$ and Notch1$^{i\Delta EC}$ livers.

Taken together, these findings lead us to propose a role for VEGFR3 dysregulation, likely through its ligand independent kinase activity, in the development of HVMs. While previous

reports have shown that inhibition of VEGFR2 ameliorates HVMs in patients(32), recent findings indicate that endothelial deletion of VEGFR2 results in decreased levels of VEGFR3(22), suggesting that targeting both VEGFR2 and the VEGFR3 activity might be the optimal strategy for the treatment of HVMs. Certainly, further studies to determine the specific role(s) of VEGFR3 and 2 signaling in the pathogenesis of HVMs are warranted.

Reduced ephrin-B2 in the Rbpj$^{i\Delta EC}$ liver suggests it may be a molecular mediator downstream of Notch signaling in HVM formation

Our results show a downregulation of *ephrin-B2* in the endothelium of Rbpj$^{i\Delta EC}$ mice, which is in agreement with previous works(6, 16, 30). Ephrin-B2 is regulated by Notch and selectively expressed in arteries(13, 18, 27). Interactions between ephrin-B2 and its receptor EphB4 are thought to segregate ECs between arteries or veins, therefore establishing arteriovenous boundaries needed for a functional vasculature(33, 34). In the liver, ephrin-B2 is expressed not only in the hepatic arteries, but also in the portal venules and the periportal sinusoids. Ephrin-B2 is likely to be involved in the establishment of porto-systemic hierarchy. In a setting where loss of function of Notch leads to increased vascular density, additional loss of ephrin-B2 would hamper an adequate establishment of vessel structure and promote the development of porto-systemic shunts.

Notch deletion may lead to HVMs in human liver

Previous studies inhibiting the Notch signaling pathway in different species have shown a highly conserved function for the Notch pathway in the liver(24), raising the possibility that inhibition of Notch signaling also results in HVMs in humans. Consistent with this, mutations in *RBPJ* and *NOTCH1* recently have been reported as the most common cause of Adams-Oliver syndrome(35, 36), a disease that presents a high frequency of vascular malformations, suggesting that perturbation of Notch signaling in the human liver also results in HVMs.

Our findings reveal an important role for Notch signaling in the development of vascular malformations in the early postnatal and adult mouse liver. Given the conservation of this signaling pathway, it is possible that disruption of Notch signaling in humans results in a similar vascular phenotype in the liver. As there are currently more than 20 ongoing clinical trials testing Notch pathway inhibitors (http://www.cancer.gov/clinicaltrials), we propose that the livers of the individuals in these trials should be diligently monitored for detrimental effects on their vasculature and function.

Supplementary Material

Refer to Web version on PubMed Central for supplementary material.

Acknowledgements

We thank Andreas Ettinger and Torsten Wittmann for assistance with and advice on cell imaging and the UCSF Liver Center for assistance with liver EC purification.

Financial support:

This research was supported by Pilot/Feasibility grant and Core facility from the UCSF Liver Center (P30 DK026743), Frank A. Campini Foundation, Vascular Cures (formerly the Pacific Vascular Research Foundation), The Cancer League, Mildred V. Strouss Trust, NIH R01 NS067420, R56NS06742, HL075033, American Heart Association grant-in-aid 10GRNT4170146 and GRNT 16850032 to R.A.W.; NIH DK59615 to V.H.S.; Tobacco-Related Disease Research Grants Program (TRDRP) Office of the University of California, Grant 20FT-0081 to H.C., TRDRP Grant 20FT-0069 and NIH F32 HL110724 to C.M.N.

List of Abbreviations

ALT	alanine transaminase
AST	aspartate transaminase
AVM	arteriovenous malformation
cv	central venule
EC	Endothelial cell
GFP	green fluorescent protein
H&E	hematoxylin and eosin
HHT	Hereditary Hemorrhagic Telangiectasia
HPF	High Power Field
HVMs	Hepatic vascular malformations
IACUC	Institutional Animal Care and Use Committee
LSEC	Liver Sinusoid Endothelial Cells
NICD	Notch intracellular domain
NRH	nodular regenerative hyperplasia
O/N	over night
P	Postnatal day
PBS	phosphate-buffered saline
pHH3	Phospho Histone H3
RT-PCR	Real time PCR
pv	portal venule
Rbpj	recombination signal binding protein for immunoglobulin kappa J region
s.e.m.	standard error of the mean
UCSF	University of California, San Francisco
VE	vascular endothelial
VEGFR	vascular endothelial growth factor receptor

REFERENCES

1. DeLeve LD, Valla DC, Garcia-Tsao G. Vascular disorders of the liver. Hepatology. 2009; 49:1729–1764. [PubMed: 19399912]
2. Gallego C, Velasco M, Marcuello P, Tejedor D, De Campo L, Friera A. Congenital and acquired anomalies of the portal venous system. Radiographics. 2002; 22:141–159. [PubMed: 11796904]
3. Guruharsha KG, Kankel MW, Artavanis-Tsakonas S. The Notch signalling system: recent insights into the complexity of a conserved pathway. Nat Rev Genet. 2012; 13:654–666. [PubMed: 22868267]
4. Hofmann JJ, Iruela-Arispe ML. Notch signaling in blood vessels: who is talking to whom about what? Circ Res. 2007; 100:1556–1568. [PubMed: 17556669]
5. Krebs LT, Xue Y, Norton CR, Shutter JR, Maguire M, Sundberg JP, Gallahan D, et al. Notch signaling is essential for vascular morphogenesis in mice. Genes Dev. 2000; 14:1343–1352. [PubMed: 10837027]
6. Dill MT, Rothweiler S, Djonov V, Hlushchuk R, Tornillo L, Terracciano L, Meili-Butz S, et al. Disruption of Notch1 induces vascular remodeling, intussusceptive angiogenesis, and angiosarcomas in livers of mice. Gastroenterology. 2012; 142:967–977. e962. [PubMed: 22245843]
7. Liu Z, Turkoz A, Jackson EN, Corbo JC, Engelbach JA, Garbow JR, Piwnica-Worms DR, et al. Notch1 loss of heterozygosity causes vascular tumors and lethal hemorrhage in mice. J Clin Invest. 2011; 121:800–808. [PubMed: 21266774]
8. Wang L, Wang CM, Hou LH, Dou GR, Wang YC, Hu XB, He F, et al. Disruption of the transcription factor recombination signal-binding protein-Jkappa (RBP-J) leads to veno-occlusive disease and interfered liver regeneration in mice. Hepatology. 2009; 49:268–277. [PubMed: 19065680]
9. Tanigaki K, Han H, Yamamoto N, Tashiro K, Ikegawa M, Kuroda K, Suzuki A, et al. Notch-RBP-J signaling is involved in cell fate determination of marginal zone B cells. Nat Immunol. 2002; 3:443–450. [PubMed: 11967543]
10. Wang Y, Nakayama M, Pitulescu ME, Schmidt TS, Bochenek ML, Sakakibara A, Adams S, et al. Ephrin-B2 controls VEGF-induced angiogenesis and lymphangiogenesis. Nature. 2010; 465:483–486. [PubMed: 20445537]
11. Muzumdar MD, Tasic B, Miyamichi K, Li L, Luo L. A global double-fluorescent Cre reporter mouse. Genesis. 2007; 45:593–605. [PubMed: 17868096]
12. Radtke F, Wilson A, Stark G, Bauer M, van Meerwijk J, MacDonald HR, Aguet M. Deficient T cell fate specification in mice with an induced inactivation of Notch1. Immunity. 1999; 10:547–558. [PubMed: 10367900]
13. Wang HU, Chen ZF, Anderson DJ. Molecular distinction and angiogenic interaction between embryonic arteries and veins revealed by ephrin-B2 and its receptor Eph-B4. Cell. 1998; 93:741–753. [PubMed: 9630219]
14. Benedito R, Hellstrom M. Notch as a hub for signaling in angiogenesis. Exp Cell Res. 2013; 319:1281–1288. [PubMed: 23328307]
15. Ehling M, Adams S, Benedito R, Adams RH. Notch controls retinal blood vessel maturation and quiescence. Development. 2013; 140:3051–3061. [PubMed: 23785053]
16. Nielsen CM, Cuervo H, Ding VW, Kong Y, Huang EJ, Wang RA. Deletion of Rbpj from postnatal endothelium leads to abnormal arteriovenous shunting in mice. Development. 2014; 141:3782–3792. [PubMed: 25209249]
17. Carlson TR, Yan Y, Wu X, Lam MT, Tang GL, Beverly LJ, Messina LM, et al. Endothelial expression of constitutively active Notch4 elicits reversible arteriovenous malformations in adult mice. Proc Natl Acad Sci U S A. 2005; 102:9884–9889. [PubMed: 15994223]
18. Murphy PA, Kim TN, Lu G, Bollen AW, Schaffer CB, Wang RA. Notch4 normalization reduces blood vessel size in arteriovenous malformations. Sci Transl Med. 2012; 4:117ra118.
19. Yao Y, Jumabay M, Wang A, Bostrom KI. Matrix Gla protein deficiency causes arteriovenous malformations in mice. J Clin Invest. 2011; 121:2993–3004. [PubMed: 21765215]

20. Li F, Lan Y, Wang Y, Wang J, Yang G, Meng F, Han H, et al. Endothelial Smad4 maintains cerebrovascular integrity by activating N-cadherin through cooperation with Notch. Dev Cell. 2011; 20:291–302. [PubMed: 21397841]
21. Tan WH, Baris HN, Burrows PE, Robson CD, Alomari AI, Mulliken JB, Fishman SJ, et al. The spectrum of vascular anomalies in patients with PTEN mutations: implications for diagnosis and management. J Med Genet. 2007; 44:594–602. [PubMed: 17526801]
22. Benedito R, Rocha SF, Woeste M, Zamykal M, Radtke F, Casanovas O, Duarte A, et al. Notch-dependent VEGFR3 upregulation allows angiogenesis without VEGF-VEGFR2 signalling. Nature. 2012; 484:110–114. [PubMed: 22426001]
23. Geisler F, Strazzabosco M. Emerging roles of Notch signaling in liver disease. Hepatology. 2015; 61:382–392. [PubMed: 24930574]
24. Yan M, Callahan CA, Beyer JC, Allamneni KP, Zhang G, Ridgway JB, Niessen K, et al. Chronic DLL4 blockade induces vascular neoplasms. Nature. 2010; 463:E6–7. [PubMed: 20147986]
25. Copeland JN, Feng Y, Neradugomma NK, Fields PE, Vivian JL. Notch signaling regulates remodeling and vessel diameter in the extraembryonic yolk sac. BMC Dev Biol. 2011; 11:12. [PubMed: 21352545]
26. Corti P, Young S, Chen CY, Patrick MJ, Rochon ER, Pekkan K, Roman BL. Interaction between alk1 and blood flow in the development of arteriovenous malformations. Development. 2011; 138:1573–1582. [PubMed: 21389051]
27. Murphy PA, Lam MT, Wu X, Kim TN, Vartanian SM, Bollen AW, Carlson TR, et al. Endothelial Notch4 signaling induces hallmarks of brain arteriovenous malformations in mice. Proc Natl Acad Sci U S A. 2008; 105:10901–10906. [PubMed: 18667694]
28. Chen W, Sun Z, Han Z, Jun K, Camus M, Wankhede M, Mao L, et al. De novo cerebrovascular malformation in the adult mouse after endothelial Alk1 deletion and angiogenic stimulation. Stroke. 2014; 45:900–902. [PubMed: 24457293]
29. Park SO, Wankhede M, Lee YJ, Choi EJ, Fliess N, Choe SW, Oh SH, et al. Real-time imaging of de novo arteriovenous malformation in a mouse model of hereditary hemorrhagic telangiectasia. J Clin Invest. 2009; 119:3487–3496. [PubMed: 19805914]
30. Krebs LT, Shutter JR, Tanigaki K, Honjo T, Stark KL, Gridley T. Haploinsufficient lethality and formation of arteriovenous malformations in Notch pathway mutants. Genes Dev. 2004; 18:2469–2473. [PubMed: 15466160]
31. Tanigaki K, Honjo T. Two opposing roles of RBP-J in Notch signaling. Curr Top Dev Biol. 2010; 92:231–252. [PubMed: 20816397]
32. Mitchell A, Adams LA, MacQuillan G, Tibballs J, vanden Driesen R, Delriviere L. Bevacizumab reverses need for liver transplantation in hereditary hemorrhagic telangiectasia. Liver Transpl. 2008; 14:210–213. [PubMed: 18236396]
33. Kim YH, Hu H, Guevara-Gallardo S, Lam MT, Fong SY, Wang RA. Artery and vein size is balanced by Notch and ephrin B2/EphB4 during angiogenesis. Development. 2008; 135:3755–3764. [PubMed: 18952909]
34. Lindskog H, Kim YH, Jelin EB, Kong Y, Guevara-Gallardo S, Kim TN, Wang RA. Molecular identification of venous progenitors in the dorsal aorta reveals an aortic origin for the cardinal vein in mammals. Development. 2014; 141:1120–1128. [PubMed: 24550118]
35. Hassed SJ, Wiley GB, Wang S, Lee JY, Li S, Xu W, Zhao ZJ, et al. RBPJ mutations identified in two families affected by Adams-Oliver syndrome. Am J Hum Genet. 2012; 91:391–395. [PubMed: 22883147]
36. Stittrich AB, Lehman A, Bodian DL, Ashworth J, Zong Z, Li H, Lam P, et al. Mutations in NOTCH1 cause Adams-Oliver syndrome. Am J Hum Genet. 2014; 95:275–284. [PubMed: 25132448]

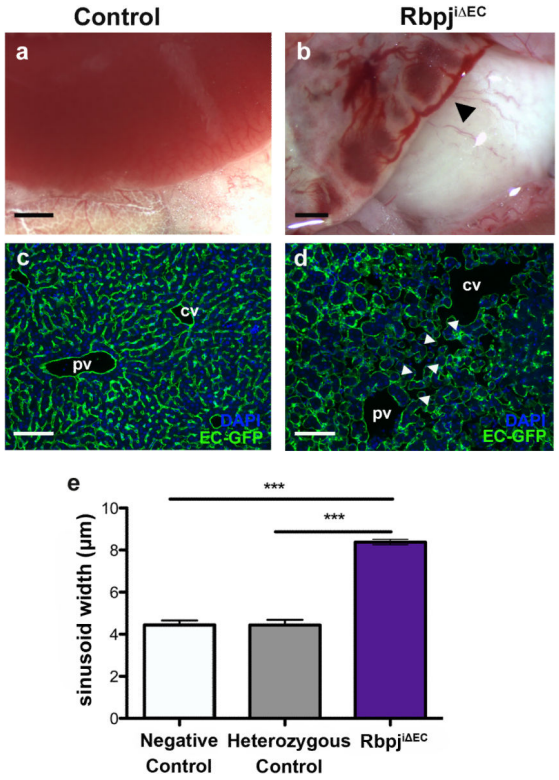

Figure 1. Endothelial specific deletion of *Rbpj* at birth led to dilated sinusoids

a,b, Liver from heterozygous control (a) and Rbpj$^{i\Delta EC}$ mutants (b) at postnatal (P) day 14 (n=47). Scale=1mm. **c,d**, Endothelial cell (EC)-mGFP expression of the *mT/mG* reporter in liver sections from control (c) and Rbpj$^{i\Delta EC}$ (d) mice. DAPI stains cell nuclei. Arrowheads indicate enlarged connections between the portal and the central venules. Scale=100μm (n=6) **e**, Sinusoid width was significantly increased in the central vein area of Rbpj$^{i\Delta EC}$. Data show mean ± s.e.m. (n=3-4 mice); ***p<0.001. p.v. portal venule, cv: central venule, EC: Endothelial Cell.

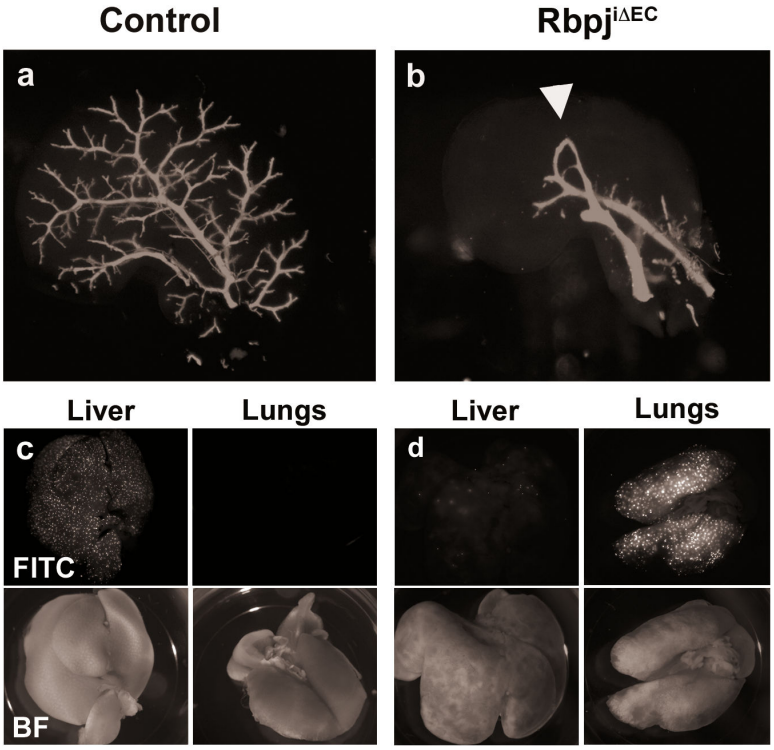

Figure 2. Endothelial specific deletion of *Rbpj* at birth resulted in liver vascular shunts

a,b, Vascular casting of control mice (a). Direct shunts were visible between the portal and central venules (arrowhead) in Rbpj$^{i\Delta EC}$ mutants (b) (n=11). **c,d**, Top, FITC-fluorescent microspheres in the liver and lungs of control (c) and Rbpj$^{i\Delta EC}$ (d) mice at P14. Below, bright field (BF) images indicate tissue orientation (n=4).

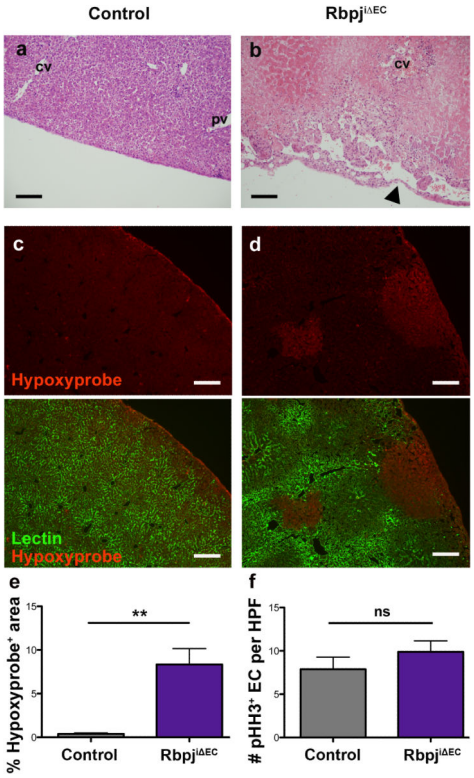

Figure 3. Immature Rbpj$^{i\Delta EC}$ mice showed increased hypoxia, poor perfusion and liver necrosis, but unaltered EC proliferation

a,b, Representative H&E images of liver sections from control (a) and Rbpj$^{i\Delta EC}$ (b) mice at P14. Arrowheads indicate enlarged subcapsular vessels connected to the central venules. (n=6). Scale=50μm. **c,d**, In contrast to controls (c), liver sections of Rbpj$^{i\Delta EC}$ mice (d) presented numerous hypoxic and poorly lectin-perfused areas. Scale=200μm. **e**, Hypoxyprobe^{+} area was significantly increased in Rbpj$^{i\Delta EC}$ mice. Data presented are mean ± s.e.m (n=3) **p<0.01. **f**, The number of pHH3^{+} ECs per HPF (high-power field) was not significantly changed in Rbpj$^{i\Delta EC}$. Data presented are mean ± s.e.m (n=7).

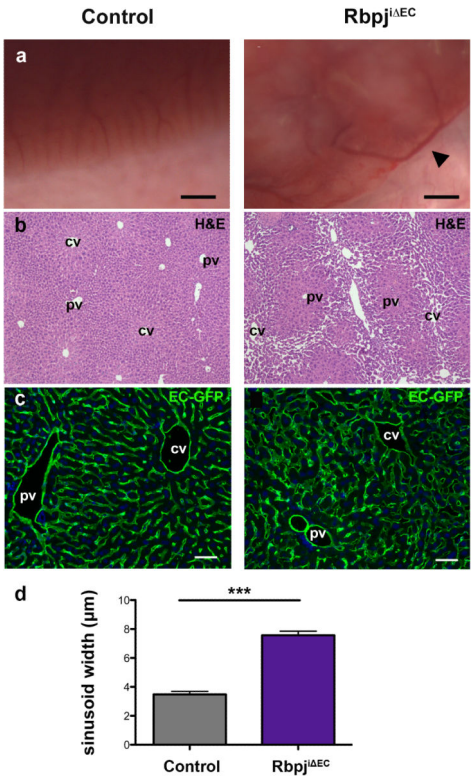

Figure 4. Adult Rbpj$^{i\Delta EC}$ mice presented dilated sinusoids

a, Liver from adult control (left panel) and Rbpj$^{i\Delta EC}$ (right panel) mice, showing enlarged vessels in mutants. (n=24). Scale=1mm. **b**, H&E staining of adult control (left panel) and Rbpj$^{i\Delta EC}$ (right panel) mice (n=5). Scale=50μm. **c**, EC-mGFP expression from the *mT/mG* reporter in liver sections. In contrast to controls (left panel), there were enlarged sinusoids between the portal and the central venules in adult Rbpj$^{i\Delta EC}$ (right panel) mice. Scale=100μm. DAPI stains cell nuclei. pv: portal venule, cv: central venule, EC: Endothelial Cell. **d**, Sinusoid width was significantly increased in the area surrounding the central vein of adult Rbpj$^{i\Delta EC}$ when compared to control littermates. Data show mean ± s.e.m. (n=3 mice); ***p<0.001.

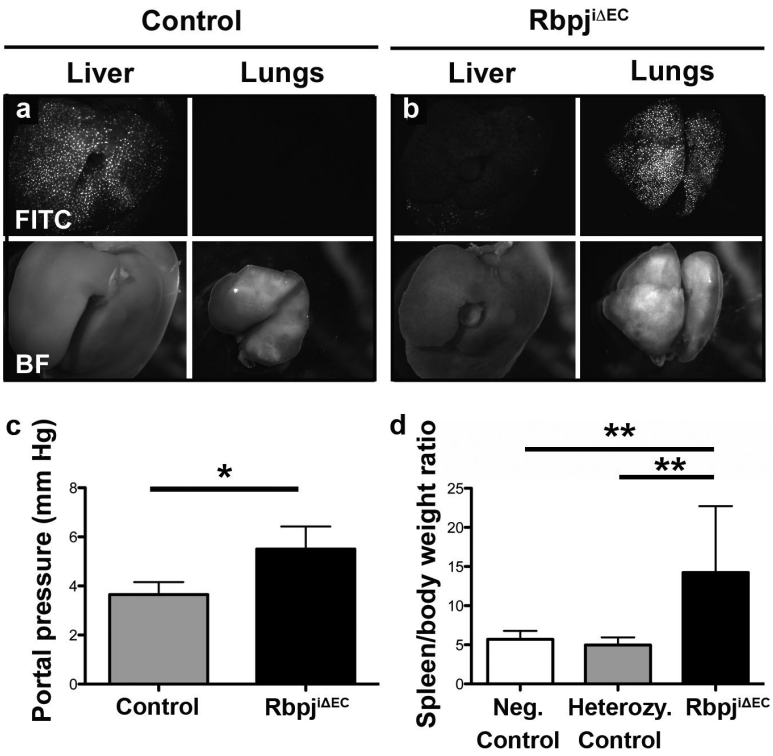

Figure 5. Adult Rbpj$^{i\Delta EC}$ mice developed liver vascular shunts and portal hypertension

a,b, Top, fluorescent microspheres in control mice (a) were retained in the liver, while in adult Rbpj$^{i\Delta EC}$ mice (b), arrested in the lung. Below, bright field (BF) images indicate tissue orientation. (n=3). **c**, Portal pressure was significantly increased in Rbpj$^{i\Delta EC}$ mice. Data show mean ± s.e.m. (n=4); *p<0.05. **d**, Spleen/body weight ratio was significantly increased in adult Rbpj$^{i\Delta EC}$ mice compared to wild-type and heterozygous controls. Data show mean ± s.e.m. (n=4-6); ** p<0.01.

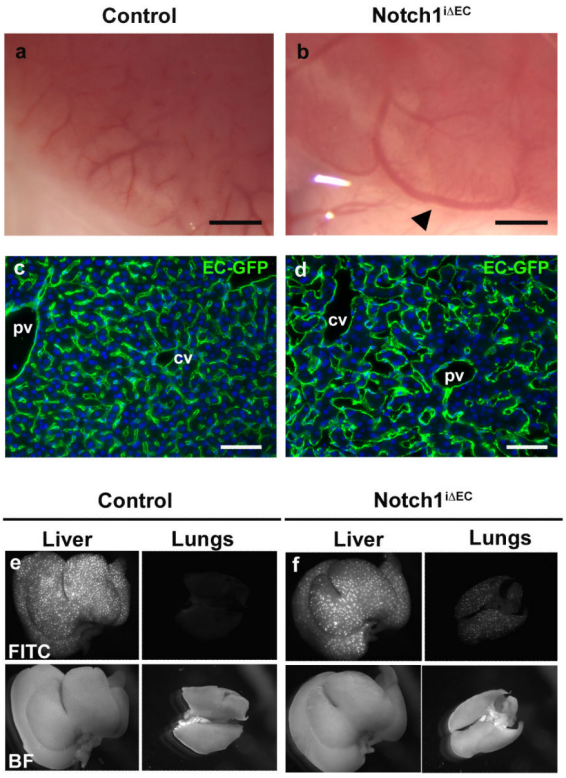

Figure 6. Endothelial deletion of *Notch1* in immature mice resulted in liver vascular shunts

a,b, Liver from control (a) and Notch1$^{i\Delta EC}$ mutant mice (a) at P14. Scale=1mm. (n=15) **c,d**, Compared to controls (c), EC-mGFP expression from the *mT/mG* reporter in Notch1$^{i\Delta EC}$ mutant (d) liver sections showed enlarged and abnormal vessels. DAPI stains cell nuclei. Scale=100μm **e,f** Top, fluorescent microspheres injected in controls (e), and Notch1$^{i\Delta EC}$ mutants (f). Below, bright field (BF) images indicate tissue orientation. (n=3). pv: portal venule, cv: central venule. EC: Endothelial Cell.

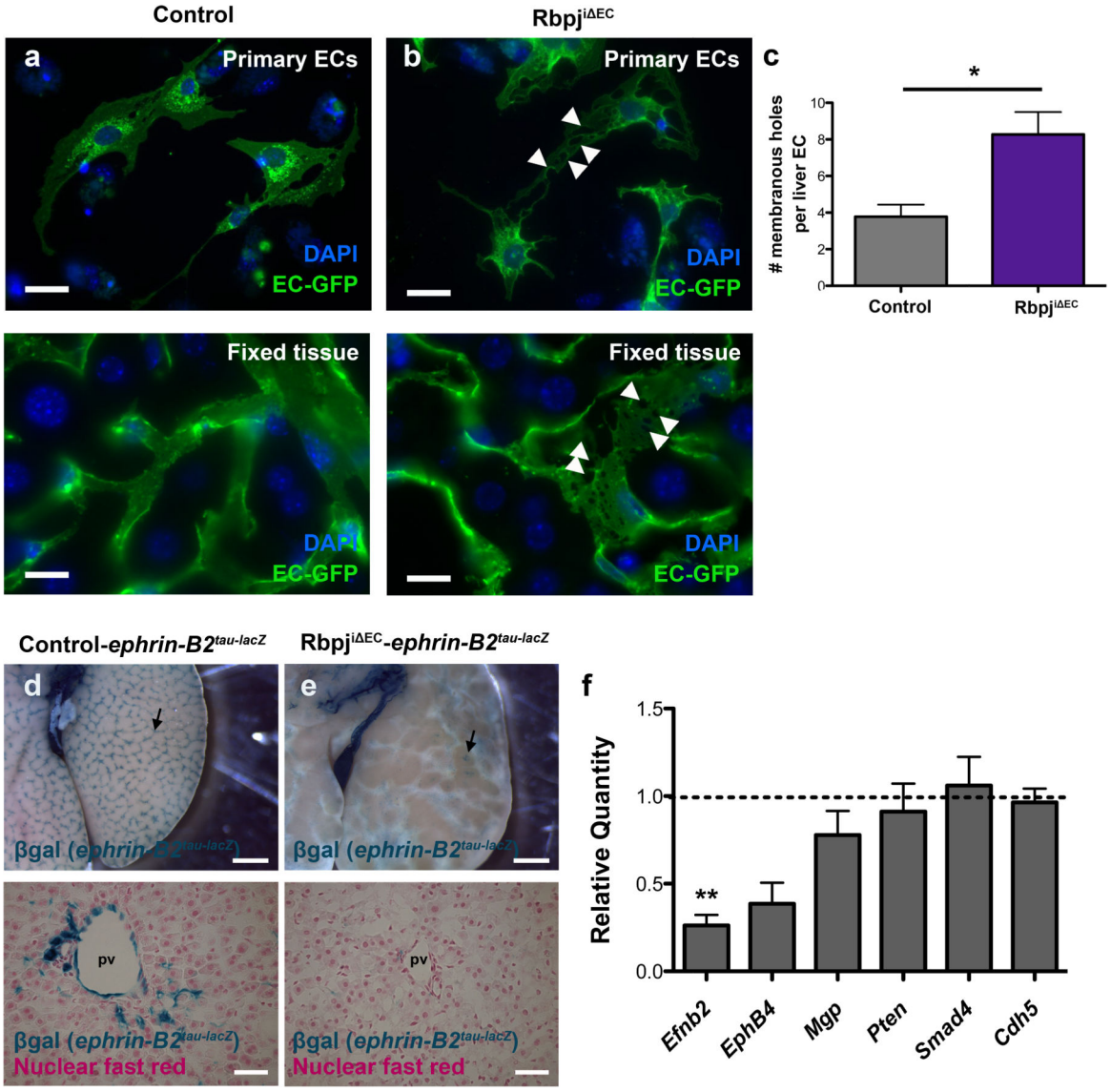

Figure 7. Primary liver ECs from Rbpj$^{i\Delta EC}$ mice exhibited aberrant cell-cell interface and decreased *ephrin-B2* expression

a,b, As compared to controls (a), liver ECs from Rbpj$^{i\Delta EC}$ mice (b), either cultured at P7 (top) or in fixed adult tissue (bottom), displayed aberrant cell-cell interface, manifesting in membranous "holes" (arrowheads). mGFP from the *mT/mG* reporter indicates ECs. DAPI stains cell nuclei. Scale=25μm. **c**, The number of membranous "holes" per P7 liver EC. Data show mean ± s.e.m. (n=3 mice); * $p<0.05$. **d,e**, *ephrin-B2$^{tau\text{-}lacZ}$* expression was decreased in P14 Rbpj$^{i\Delta EC}$ liver (e), as compared to controls (d). *ephrin-B2$^{tau\text{-}lacZ}$* expression is shown in whole liver (top panels in d,e) and in liver sections (bottom panels in d,e). Nuclear fast red stains nuclei. Scale=1mm (top panels in d,e); 25μm (bottom panels in d,e). **f**, Quantitative RT-PCR analysis of P7 liver ECs. Data are presented as mean ± s.e.m. (n=3). * $p<0.05$.

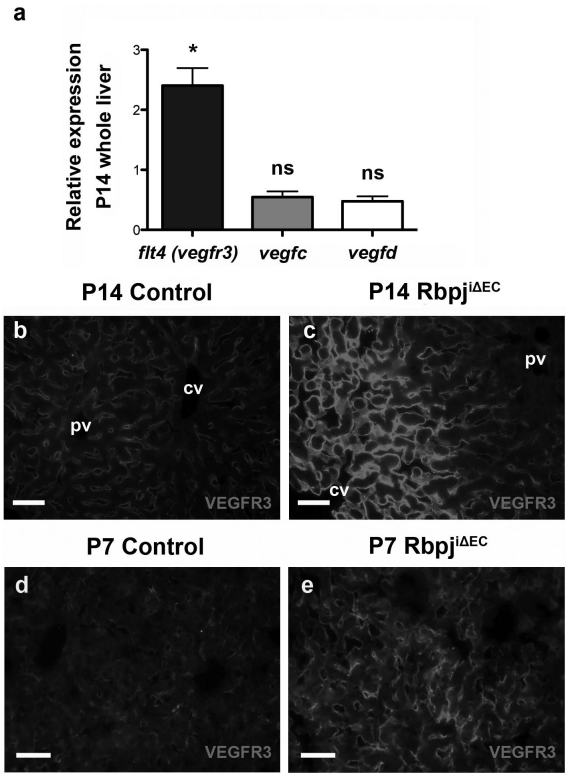

Figure 8. VEGFR3, but not *vegfc* or *vegfd*, was upregulated in Rbpj$^{i\Delta EC}$ mice

a, Quantitative RT-PCR analysis of P14 whole liver tissue. Data are presented as mean ± s.e.m. (n=3). * p <0.05. **b,c,d,e** VEGFR3 immunostaining in liver sections control (b,d) and Rbpj$^{i\Delta EC}$ (c,e) mice indicated an increase in VEGFR3 in P14 (c) and P7 (e) mutants. Scale=50μm. (n=4) pv: portal venule, cv: central venule.